Nonlinear Dyn (2013) 74:439–453
DOI 10.1007/s11071-013-0981-x

ORIGINAL PAPER

A new study of chaotic behavior and the existence of Feigenbaum's constants in fractional-degree *Yin–Yang* Hénon maps

Chun-Yen Ho · Hsien-Keng Chen · Zheng-Ming Ge

Received: 8 September 2012 / Accepted: 11 June 2013 / Published online: 1 August 2013

Abstract In this paper, we firstly develop fractional-degree Hénon maps with increasing and decreasing argument n. *Yin* and *Yang* are two fundamental opposites in Chinese philosophy. *Yin* represents the moon and is the decreasing, negative, historical, or feminine principle in nature, while *Yang* represents the sun and is the increasing, positive, contemporary, or masculine principle in nature. Chaos produced by increasing n is called *Yang* chaos, that by decreasing n *Yin* chaos, respectively. The simulation results show that chaos appears via positive Lyapunov exponents, bifurcation diagrams, and phase portraits. In order to examine the existence of chaotic behaviors in fractional-degree *Yin–Yang* Hénon maps, Feigenbaum's constants are measured in this paper. It is found that the Feigenbaum's constants in fractional-degree *Yin–Yang* Hénon maps are of great precision to the first and second Feigenbaum's constants. A detailed analysis of the chaotic behaviors is also performed for the fractional-degree Hénon maps with increasing (*Yang*) and decreasing (*Yin*) argument n.

C.-Y. Ho · Z.-M. Ge (✉)
Department of Mechanical Engineering,
National Chiao Tung University, 1001 Ta Hsueh Road,
Hsinchu 300, Taiwan
e-mail: zmg@cc.nctu.edu.tw

H.-K. Chen
Department of Mechanical Engineering,
Hsiuping University of Science and Technology,
11 Gongye Rd., Dali Dist., Taichung 412-80, Taiwan

Keywords Chinese philosophy · *Yin* chaos · *Yang* chaos · Hénon maps · Feigenbaum's constants · Fractional-degree *Yin–Yang* chaos

1 Introduction

Chaos, as an interesting nonlinear phenomenon, has been intensively investigated in the last three decades [1–8]. It is well known that chaotic systems have sensitive dependence on initial conditions, and chaotic behaviors have become an important research subject in nonlinear sciences [9–13]. These nonlinear phenomena have been applied in many fields, such as secure communication [14–18], chemical reactions [19], and biological systems [20]. Chaos exists in both continuous and discrete nonlinear systems. Hénon map [21–23], is the classical, well-known discrete nonlinear systems, and its chaotic behaviors have been studied via a large number of researchers.

I Ching, is known as the Classic of Changes, is the first of the Five Classics in Chinese culture. It is a collection of ethical experiences from ancient people and has been used as a guide of being a good person. On the meaning of the name *I Ching*, it is an ancient document that describes the philosophy of the universe via the changes of the moon and the sun. The moon and the sun are represented as *Yin* and *Yang*, respectively.

In 1975, Feigenbaum discovered two constants, which are called Feigenbaum's constants δ and α, where $\delta = 4.66920\ldots$, and $|\alpha| = 2.5029\ldots$ when

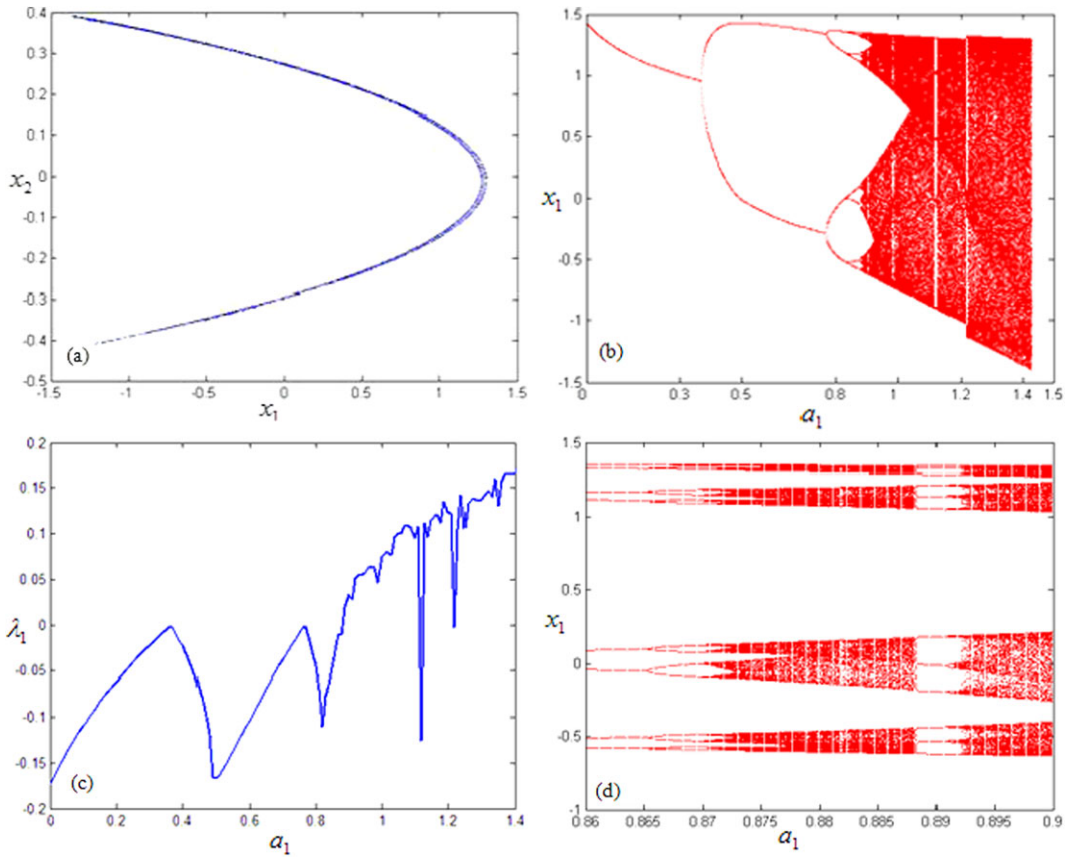

Fig. 1 The fractional-degree *Yang* Hénon map with $q_1 = q_2 = 1$, $b_1 = 0.3$: (**a**) phase portrait with $a_1 = 1.4$, bifurcation diagrams with a_1 is varied: (**b**) $0 \leq a_1 \leq 1.5$, (**d**) $0.86 \leq a_1 \leq 0.9$, (**c**) the largest Lyapunov exponent with $a_1 = 0 \sim 1.4$

Table 1 Bifurcation points for each case

Case	q_1	q_2	$a(1)$	$a(2)$	$a(3)$	$a(4)$	$a(5)$	$a(6)$
1	1	1	0.368042	0.769134	0.849731	0.866331	0.869884	0.870645
2	0.99	1.9	0.579137	1.099208	1.219609	1.246652	1.252507	1.253753
3	0.9	1	0.429799	0.805855	0.869892	0.882955	0.885755	0.886355
4	1	0.9	0.368252	0.720598	0.785837	0.799428	0.802341	0.802965
5	0.98	0.98	0.373616	0.767808	0.84597	0.86194	0.865362	0.866095
6	0.94	0.94	0.38549	0.766374	0.834148	0.84875	0.851875	0.852544
7	1	1	1.267114	1.846424	1.951662	1.972614	1.977059	1.978011
8	0.99	1.9	0.917653	1.387428	1.501890	1.527159	1.532665	1.533842
9	0.9	1	1.233279	1.724023	1.827632	1.849776	1.854514	1.855529
10	1	0.9	1.344044	1.962335	2.061627	2.081358	2.085490	2.086375
11	0.98	0.98	1.281236	1.842318	1.94647	1.967451	1.972007	1.972982
12	0.94	0.94	1.309129	1.833289	1.934771	1.955761	1.960208	1.961156

Table 2 Measurement results of Feigenbaum's constants and errors for each case

Case	i	δ_i	Percentage error of δ_i	$\lvert\alpha_i\rvert$	Percentage error of $\lvert\alpha_i\rvert$
1	1	4.976512	6.581 %	3.034366	21.23 %
	2	4.855240	3.984 %	2.848865	13.82 %
	3	4.672108	0.062 %	2.570944	2.718 %
	4	4.668856	0.007 %	2.501618	0.051 %
2	1	4.319490	7.489 %	2.793279	11.6 %
	2	4.452205	4.647 %	2.542469	1.58 %
	3	4.618787	1.079 %	2.519736	0.67 %
	4	4.699036	0.638 %	2.507169	0.17 %
3	1	5.417083	16.01 %	3.174695	26.84 %
	2	5.226943	11.94 %	2.906941	16.14 %
	3	4.99557	6.989 %	2.532188	1.17 %
	4	4.666666	0.054 %	2.503681	0.03 %
4	1	5.043269	8.011 %	3.149333	25.82 %
	2	4.894301	4.820 %	2.810731	12.29 %
	3	4.666861	0.050 %	2.500140	0.11 %
	4	4.668485	0.015 %	2.501854	0.041 %
5	1	5.043269	8.011 %	3.149333	25.82 %
	2	4.894301	4.820 %	2.810731	12.29 %
	3	4.666861	0.050 %	2.500140	0.11 %
	4	4.668485	0.015 %	2.501854	0.041 %
6	1	5.372258	15.057 %	3.202252	27.94 %
	2	4.821805	3.268 %	2.716627	8.53 %
	3	4.672640	0.073 %	2.511764	0.35 %
	4	4.671150	0.041 %	2.503639	0.029 %
7	1	5.504760	17.895 %	2.582036	3.16 %
	2	5.022814	7.573 %	2.55625	2.13 %
	3	4.713610	0.951 %	2.529411	1.059 %
	4	4.669117	0.001 %	2.5	0.11 %
8	1	4.104200	12.100 %	2.738127	9.39 %
	2	4.529740	2.986 %	2.454444	1.93 %
	3	4.589357	1.710 %	2.492268	0.42 %
	4	4.677994	0.188 %	2.505338	0.097 %
9	1	4.736499	1.441 %	3.039444	21.43 %
	2	4.678874	0.207 %	2.810799	12.3 %
	3	4.673701	0.096 %	2.516620	0.54 %
	4	4.667980	0.026 %	2.505288	0.095 %
10	1	6.226997	33.363 %	2.559420	2.25 %
	2	5.032284	7.776 %	2.530434	1.1 %
	3	4.775169	2.269 %	2.5	0.11 %
	4	4.668926	0.005 %	2.504878	0.079 %
11	1	5.387145	15.376 %	2.731021	9.11 %
	2	4.964110	6.316 %	2.602681	3.98 %
	3	4.605136	1.372 %	2.508035	0.205 %
	4	4.672820	0.077 %	2.505307	0.096 %

Table 2 (*Continued*)

Case	i	δ_i	Percentage error of δ_i	$\lvert\alpha_i\rvert$	Percentage error of $\lvert\alpha_i\rvert$
12	1	5.165053	10.619 %	2.776734	10.94 %
	2	4.834778	3.546 %	2.657534	6.17 %
	3	4.720035	1.088 %	2.517241	0.572 %
	4	4.690928	0.465 %	2.502720	0.007 %

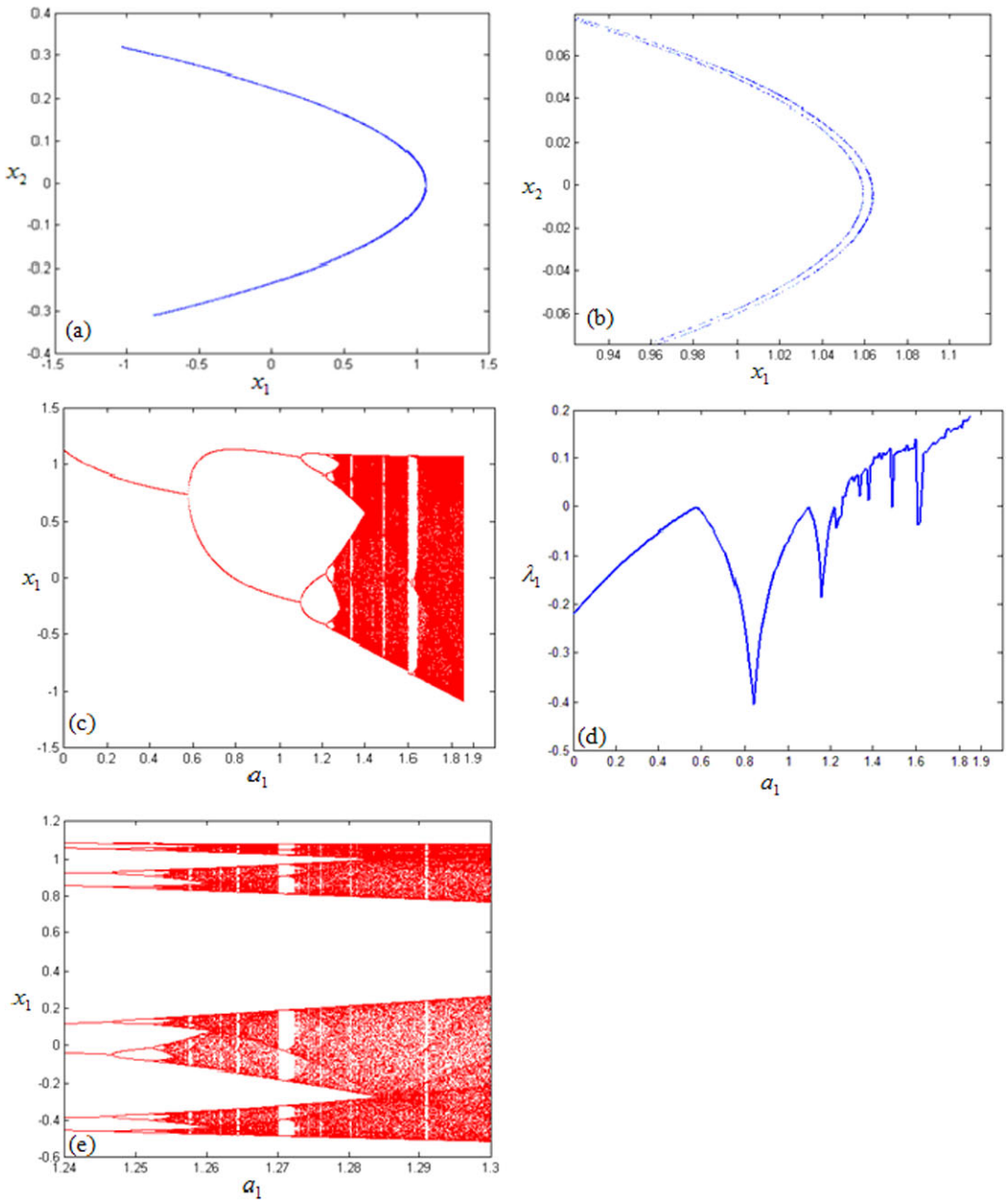

Fig. 2 The fractional-degree *Yang* Hénon map with $q_1 = 0.9$, $q_2 = 1.99$, $b_1 = 0.3$: (**a**), (**b**) phase portrait with $a_1 = 1.8$, bifurcation diagrams with a_1 is varied: (**c**) $0 \leq a_{1\leq} 1.9$, (**e**) $1.24 \leq a_{1\leq} 1.3$. (**d**) the largest Lyapunov exponent with $a_1 = 0 \sim 1.9$

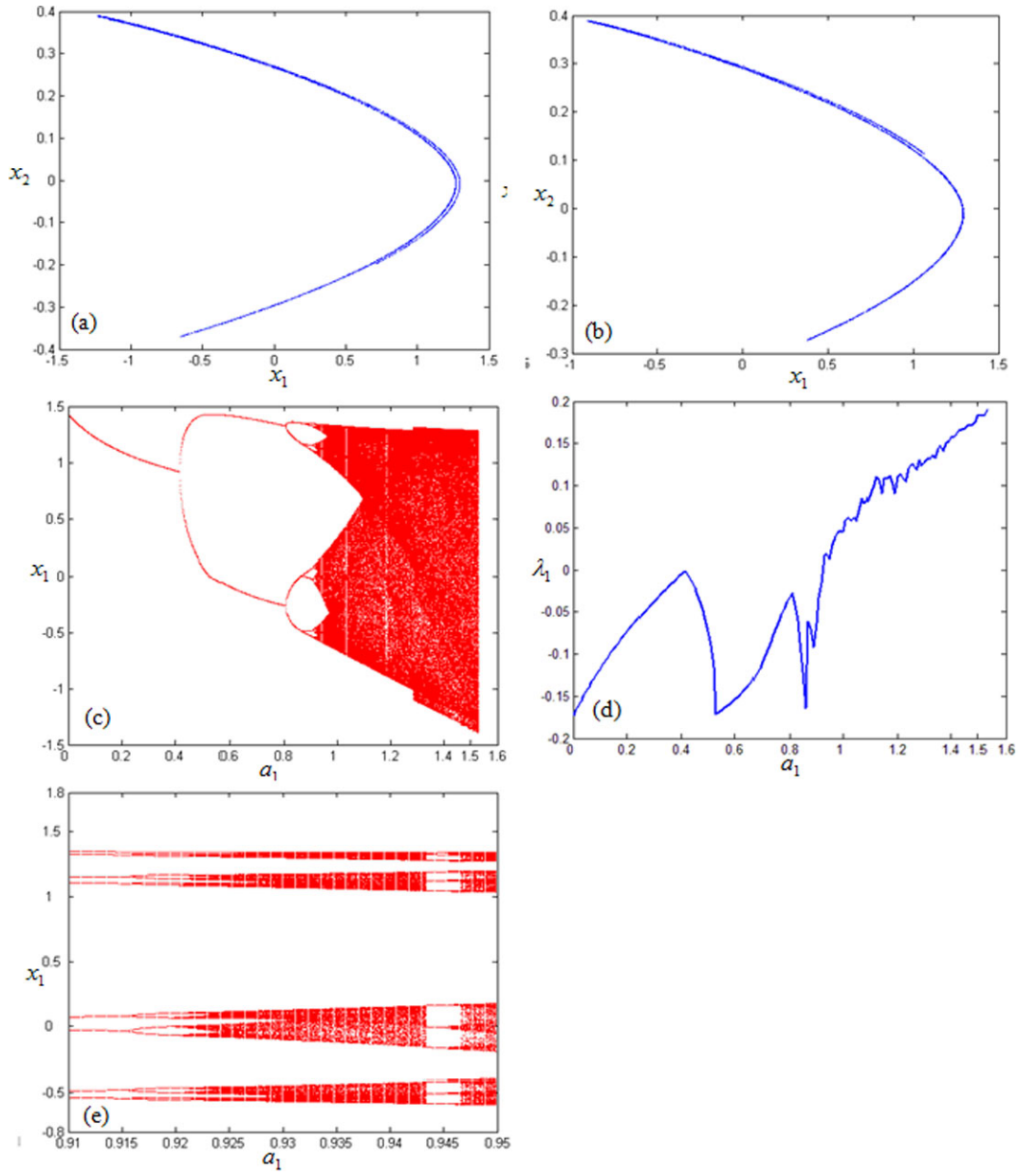

Fig. 3 The fractional-degree *Yang* Hénon map with $q_1 = 0.9$, $q_2 = 1$, $b_1 = 0.3$: (**a**) phase portrait with $a_1 = 1.4$, (**b**) phase portrait with $a_1 = 1.2$. Bifurcation diagrams with a_1 is varied: (**c**) $0 \leq a_1 \leq 1.6$ (**e**) $0.91 \leq a_1 \leq 0.95$ (**d**) the largest Lyapunov exponent with $a_1 = 0 \sim 1.6$

the dynamical system approaches chaotic behavior via period-doubling bifurcation [24]. Feigenbaum's constants were found in many chaotic systems [25–29]. The measurement of Feigenbaum's constants in a continuous time fractional-order system was firstly performed in detail by Chen et al. [29]. Ge and Li [30] investigated the dynamics of continuous time chaotic system with negative time and the chaotic behavior of continuous time nonlinear system with negative time is called "*Yin* chaos." Contrarily, the classical positive time counterpart is called "*Yang* chaos." Ho, Chen, and Ge [31] investigated *Yin* and *Yang* chaos of discrete time maps. In order to make the research of *Yin* and *Yang* chaos more complete, we firstly study the *Yin* and

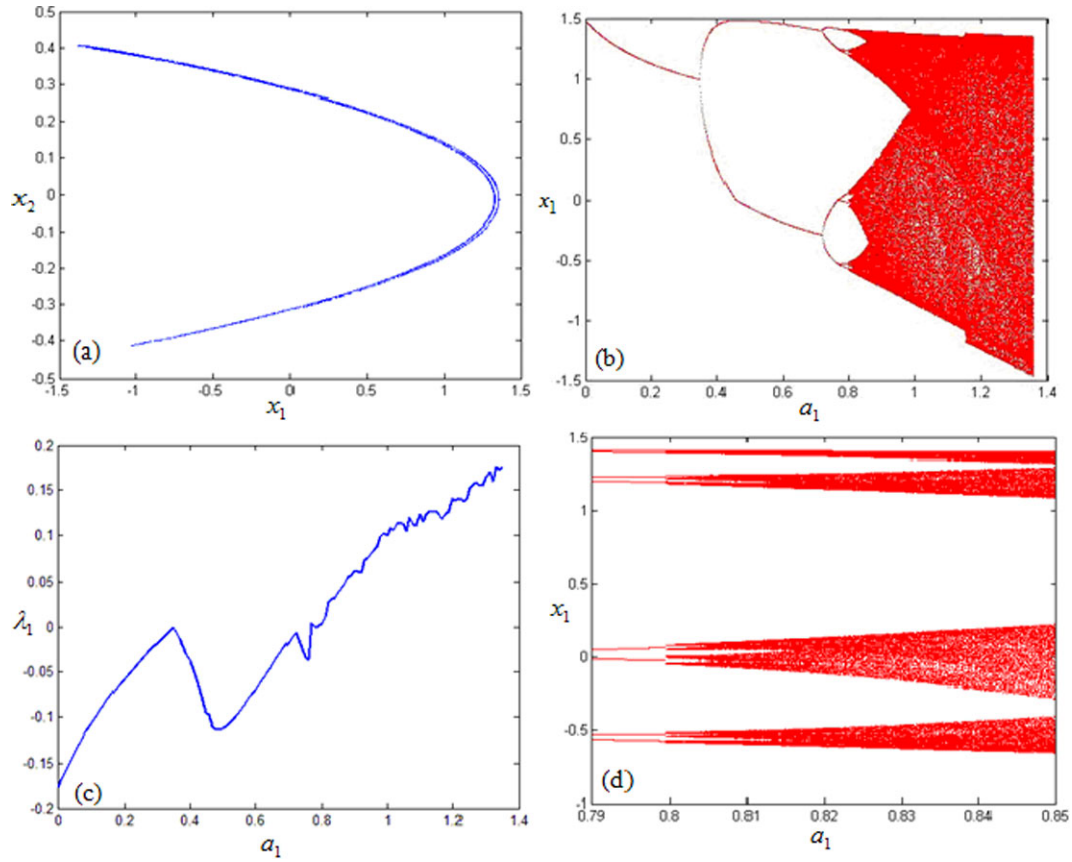

Fig. 4 The fractional-degree *Yang* Hénon map with $q_1 = 1$, $q_2 = 0.9$, $b_1 = 0.3$: (**a**) phase portrait with $a_1 = 1.3$. Bifurcation diagrams with a_1 is varied: (**b**) $0 \leq a_{1\leq} 1.4$ (**d**) $0.79 \leq a_{1\leq} 0.85$ (**c**) the largest Lyapunov exponent with $a_1 = 0 \sim 1.4$

Yang chaos that appeared in fractional-degree maps. Meanwhile, the Feigenbaum's constants in this fractional degree map are also measured.

This paper is organized as follows: The fractional-degree *Yang* and *Yin* Hénon maps are introduced in Sect. 2, together with a review of the definition of the first and second Feigenbaum's constants. The chaos characteristics of the two maps are analyzed using Lyapunov spectra, phase portraits, and bifurcation diagrams in Sect. 3. The measurement of Feigenbaum's constants of the two maps is carried out in the same section. Finally, conclusions are drawn in Sect. 4.

2 Chaos of fractional-degree *Yin–Yang* Hénon maps

The research of Hénon map extends to a new era by replacing the integer degrees to fractional ones. Two novel fractional-degree Hénon maps are introduced in the following. Moreover, the definition of Feigenbaum's constants is reviewed in this section.

2.1 Fractional-degree *Yang* Hénon map

The equations of the fractional-degree *Yang* Hénon map with increasing n_1 are described as follows:

$$\begin{aligned} x_1[n_1+1] &= -a_1 \left\| x_1^{2q_1}[n_1] \right\| + \left\| x_2^{q_2}[n_1] \right\| + 1 \\ x_2[n_1+1] &= b_1 x_1[n_1] \end{aligned} \tag{1}$$

where $\|\cdot\|$ is the norm of a complex number, $a_1, b_1 \in R$ are the system parameters, q_1 and q_2 are positive real numbers, $n_1 = 0, 1, 2, 3, \ldots, n$, n is a nonnegative integer sequence, x_1 and x_2 are the states of the map. The initial conditions are chosen to be $\{x_1[0], x_2[0]\} = \{0.63, 0.19\}$, and b_1 is fixed as $b_1 = 0.3$ throughout the paper.

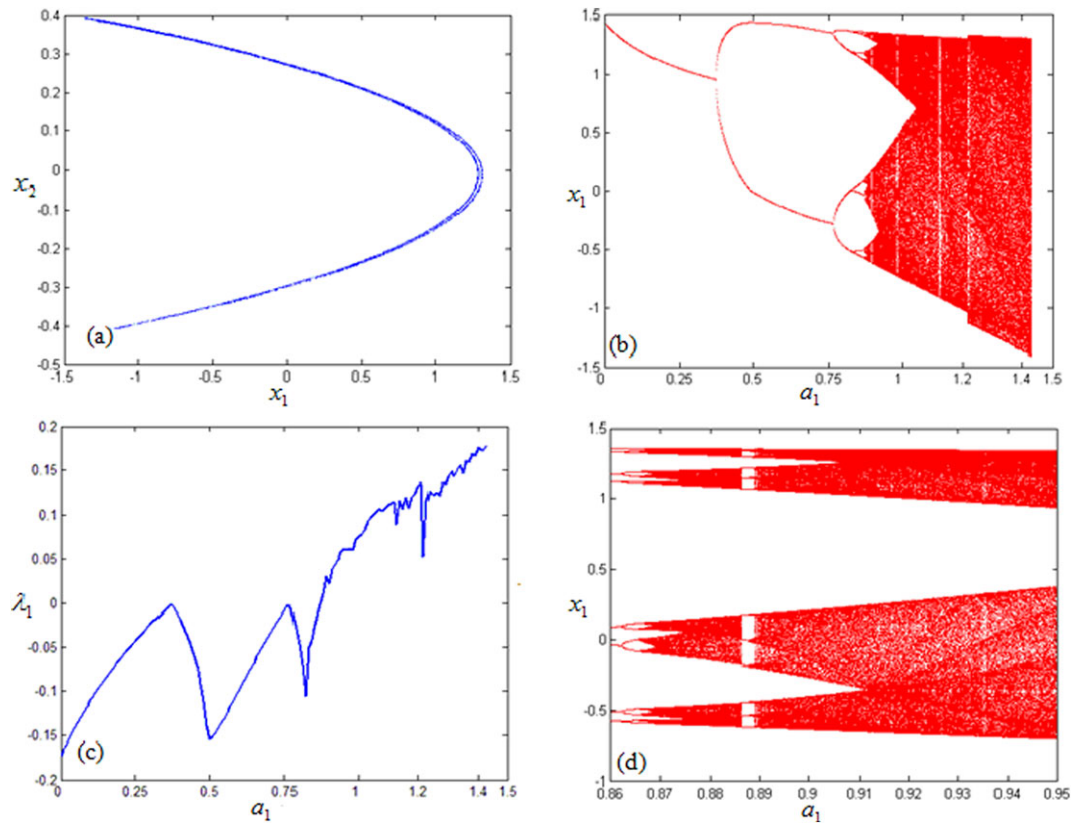

Fig. 5 The fractional-degree *Yang* Hénon map with $q_1 = q_2 = 0.98$, $b_1 = 0.3$: (**a**) phase portrait with $a_1 = 1.4$. Bifurcation diagrams with a_1 is varied: (**b**) $0 \leq a_1 \leq 1.5$ (**d**) $0.86 \leq a_1 \leq 0.95$ (**c**) the largest Lyapunov exponent with $a_1 = 0 \sim 1.5$

2.2 Fractional-degree *Yin* Hénon map

The fractional-degree *Yin* Hénon map with decreasing n_2 is defined as

$$\begin{aligned} y_1[n_2 - 1] &= b_2 y_2[n_2] \\ y_2[n_2 - 1] &= a_2 \left\| y_2^{2q_1}[n_2] \right\| + \left\| y_1^{q_2}[n_2] \right\| - 1 \end{aligned} \tag{2}$$

where a_2, $b_2 \in R$, and $b_2 = 0.3$ are the system parameters, q_1 and q_2 are positive real numbers, $n_2 = -1, -2, -3, \ldots, -n$, $-n$ is a nonpositive integer sequence, y_1 and y_2 are the states of the map. The initial conditions are set as $\{y_1[0], y_2[0]\} = \{0.19, 0.63\}$.

2.3 The first and second Feigenbaum's constants

The first Feigenbaum's constant δ is defined in [24] as

$$\delta = \lim_{i \to \infty} \frac{a_{i+1} - a_i}{a_{i+2} - a_{i+1}} \tag{3}$$

where a_i is the value of the parameter at the ith bifurcation point, and the value of δ is $4.66920\ldots$.

The second Feigenbaum's constant $|\alpha|$ is defined as

$$|\alpha| = \left| \frac{\Delta M_{x_i}}{\Delta M_{x_{i+1}}} \right| \tag{4}$$

where ΔM_{x_i} is the width of the widest bifurcation fork of ith bifurcation, and $|\alpha| = 2.5029\ldots$.

3 Chaotic behaviors and measurement of Feigenbaum's constants

In this section, the measurement of the first and second Feigenbaum's constants and various chaotic behaviors are studied on different types of q_1, q_2. The fractional-degree *Yang* Hénon map is analyzed in the first 6 cases, and the *Yin* Hénon map in the remaining 6 cases.

These 12 cases of q_1, q_2 can be classified as:

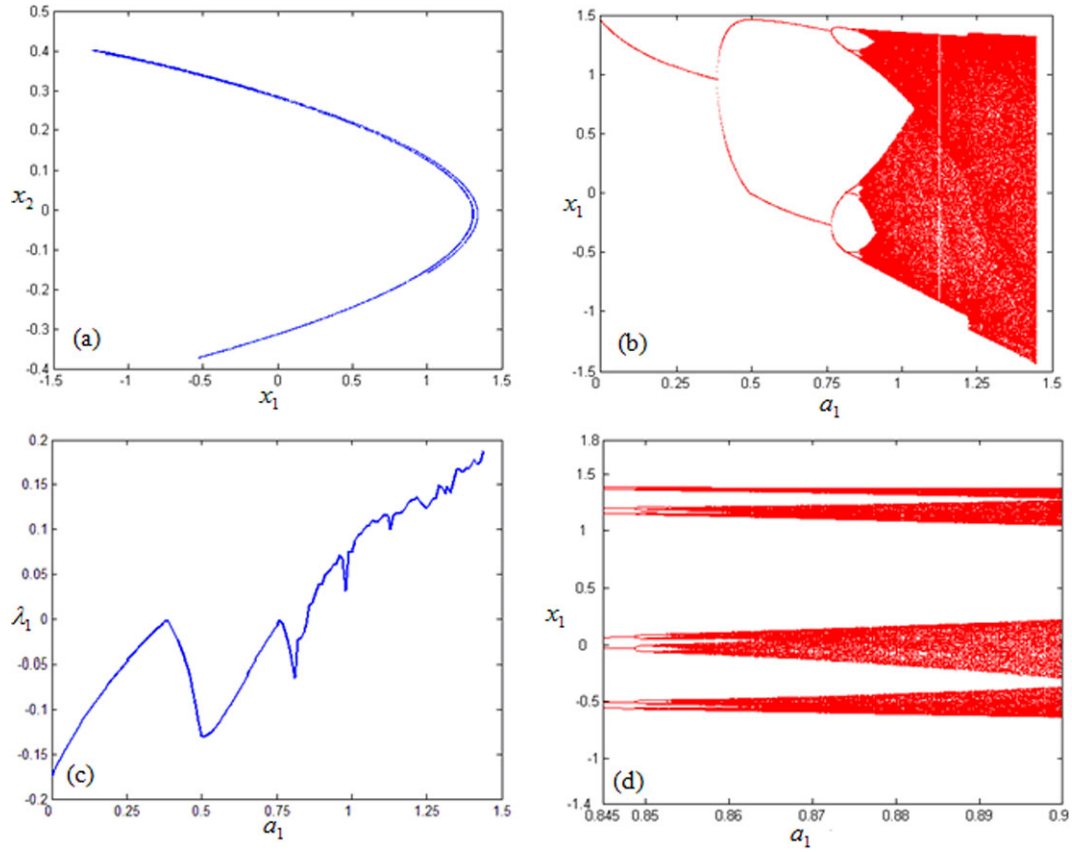

Fig. 6 The fractional-degree *Yang* Hénon map with $q_1 = q_2 = 0.94$, $b_1 = 0.3$: (**a**) phase portrait with $a_1 = 1.4$. Bifurcation diagrams with a_1 is varied: (**b**) $0 \leq a_1 \leq 1.5$ (**c**) the largest Lyapunov exponent with $a_1 = 0 \sim 1.5$

Case 1, 7: q_1, q_2 are integer degree.
Case 2, 8: q_1, q_2 are different fractional degree.
Case 3, 9: q_1 is fractional degree and q_2 is integer degree.
Case 4, 10: q_1 is integer degree and q_2 is fractional degree.

Case 5, 6, 11, and 12: q_1, q_2 are same fractional degree.

The values of a at the ith bifurcation point are shown in Table 1, where $i = 1, 2, 3 \ldots, 6$. The first and second Feigenbaum's constants can be calculated by Table 1. The measurement results of the first and second Feigenbaum's constants for these 12 cases are listed in Table 2.

3.1 Case 1 *Yang* Hénon map with $q_1 = q_2 = 1$

In this case, the q_1, q_2 are integer degree and the numerical results are shown in Figs. 1. A phase portrait is plotted in Fig. 1(a), where $a_1 = 1.4$. Figure 1(b) and (d) are the bifurcation diagrams of x_1, which can be shown the period-doubling bifurcations clearly. The largest Lyapunov exponent for $a_1 = 0$ to 1.5 is shown in Fig. 1(c). The dynamics approaches to infinity when $a_1 > 1.426$.

The measurement results of the first and second Feigenbaum's constants for $i = 1$, 2, 3, and 4 are shown in Table 2. It is shown that measurement values of the first and second Feigenbaum's constants are great precision to 4.66920... with error percentage 0.007 % and 2.5029... with error percentage 0.051 %, respectively when $i = 4$. More detailed measurement results of δ and $|\alpha|$ for $i = 1$, 2, 3 are shown in Table 2.

3.2 Case 2 *Yang* Hénon map with $q_1 = 0.99$, $q_2 = 1.9$

By setting $q_1 = 0.99$, $q_2 = 1.9$ in Eq. (1), the numerical results of the fractional-degree *Yang* Hénon

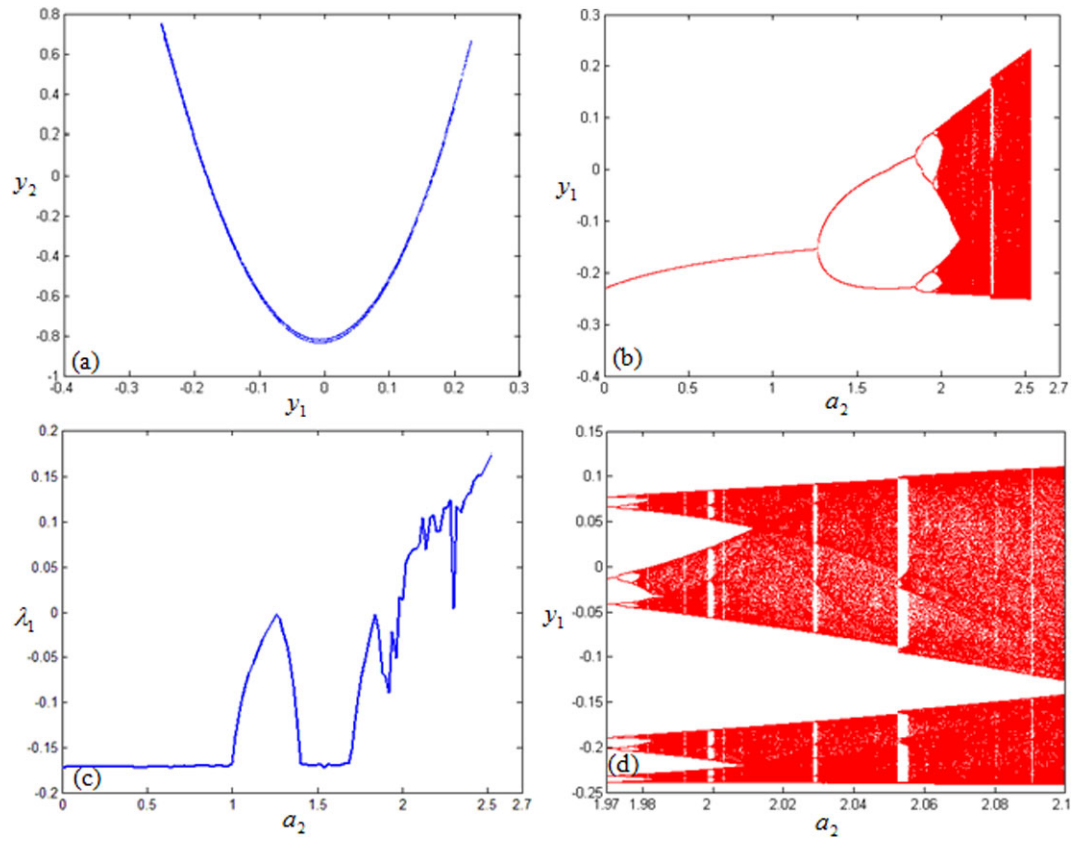

Fig. 7 The fractional-degree *Yin* Hénon map with $q_1 = q_2 = 1$, $b_2 = 0.3$: (**a**) phase portrait with $a_2 = 2.5$. Bifurcation diagrams with a_2 is varied: (**b**) $0 \le a_2 \le 2.7$ (**d**) $1.97 \le a_2 \le 2.1$ (**c**) the largest Lyapunov exponent with $a_2 = 0 \sim 2.7$

map are shown in Figs. 2. A phase portrait is plotted in Fig. 2(a), where $a_1 = 1.8$. Comparing with this case and case 1, it is found that the chaotic behavior of this case is squeezed so that the motion is similar to a parabola pattern (Fig. 2(a)), where Fig. 2(b) shows an enlarged view of Fig. 2(a). A more complicated chaotic behavior can be seen in the bifurcation diagrams of x_1 in Figs. 2(c) and (e). The largest Lyapunov exponent for $a_1 = 0$ to 1.9 is shown in Fig. 2(d). Various dynamic behaviors for varied a_1 are shown in Figs. 2(c) and (d), such as the period-3 when $1.602 \le a_1 \le 1.616$, and the dynamics approaches to infinity when $a_1 > 1.855$.

The first Feigenbaum's constant measures $\delta = 4.699036$, with an error percentage of 0.63 % when $i = 4$. The second Feigenbaum's constant measures $|\alpha| = 2.5071692$, with an error percentage of 0.17 % when $i = 4$.

3.3 Case 3 *Yang* Hénon map with $q_1 = 0.9$, $q_2 = 1$

By setting $q_1 = 0.9$, $q_2 = 1$ to the *Yang* Hénon map, the numerical results of the fractional-degree *Yang* Hénon map are shown in Figs. 3. Figure 3(a) and (b) show the chaotic motion for $a_1 = 1.4$ and $a_1 = 1.2$, respectively. It is clearly shown that the chaotic motion of Fig. 3(a) expands wider than Fig. 3(b). Figure 3(c) and (e) are the bifurcation diagrams of x_1. The largest Lyapunov exponent for a_1 from 0 to 1.6 is shown in Fig. 3(d). The dynamics approaches to infinity when $a_1 > 1.523$.

The first Feigenbaum's constant measures $\delta = 4.666666$, with an error percentage of 0.054 % when $i = 4$. The second Feigenbaum's constant measures $|\alpha| = 2.503681$, with an error percentage of 0.03 % when $i = 4$.

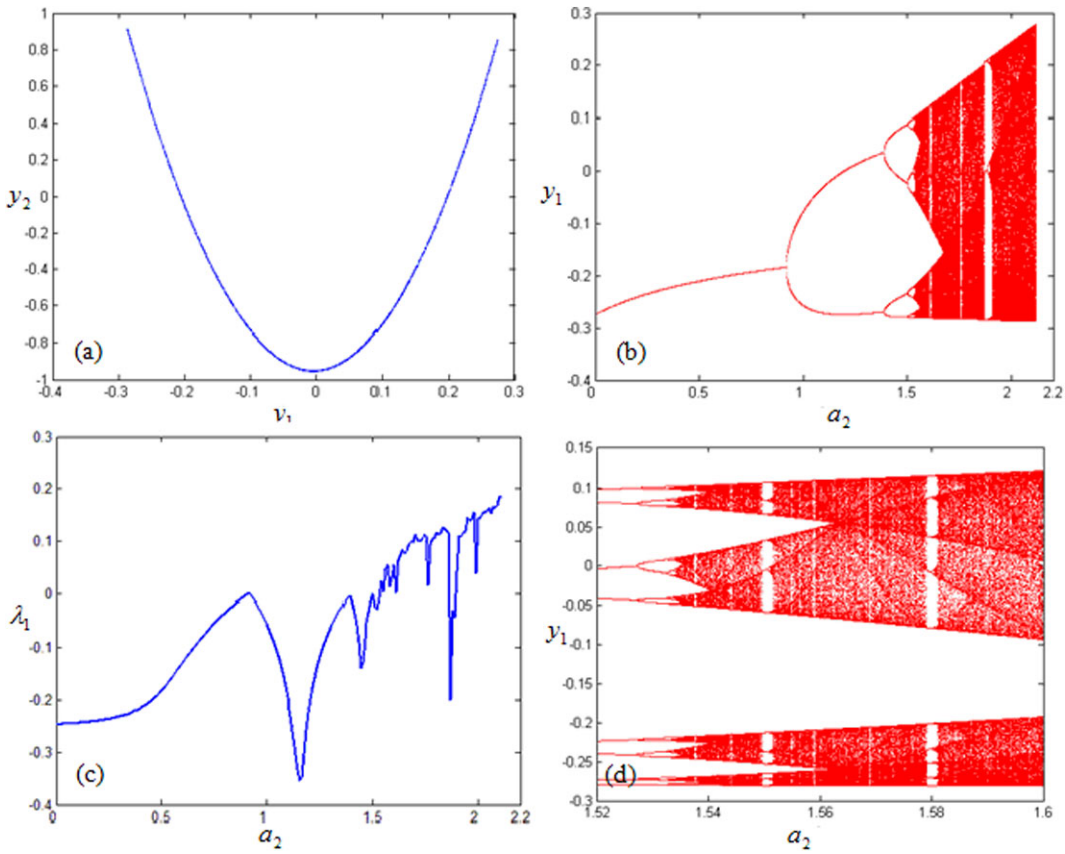

Fig. 8 The fractional-degree *Yin* Hénon map with $q_1 = 0.99$, $q_2 = 1.9$, $b_2 = 0.3$: (**a**) phase portrait with $a_2 = 2.1$. Bifurcation diagrams with a_2 is varied: (**b**) $0 \leq a_{2\leq} 2.2$ (**d**) $1.52 \leq a_{2\leq} 1.6$ (**c**) the largest Lyapunov exponent with $a_2 = 0 \sim 2.2$

3.4 Case 4 *Yang* Hénon map with $q_1 = 1$, $q_2 = 0.9$

By setting $q_1 = 1$, $q_2 = 0.9$ in Eq. (1), the numerical results of the fractional-degree *Yang* Hénon map are shown in Figs. 4. A phase portrait is plotted in Fig. 4(a), where $a_1 = 0.3$. The bifurcation diagrams of x_1 are shown in Figs. 4(b) and (d). The largest Lyapunov exponent is shown in Fig. 4(c). The dynamics approaches to infinity when $a_1 > 1.351$.

Feigenbaum's constant measure 4.668269 and 2.504215, having error percentage of 0.02 % and 0.05 % when $i = 4$.

3.5 Case 5 *Yang* Hénon map with $q_1 = q_2 = 0.98$

By setting $q_1 = q_2 = 0.98$ in Eq. (1), the numerical results of the fractional-degree *Yang* Hénon map are shown in Figs. 5. A phase portrait is plotted in Fig. 5(a), where $a_1 = 1.4$. Figure 5(b) and (d) are the bifurcation diagrams of x_1. The largest Lyapunov exponent for varied $a_1 = 0$ to 1.5 is shown in Fig. 5(c). The dynamics approaches to infinity when $a_1 > 1.434$.

The first Feigenbaum's constant measures $\delta = 4.668485$, with an error percentage of 0.015 % and the second Feigenbaum's constant measures $|\alpha| = 2.5018542$, with an error percentage of 0.04 % when $i = 4$.

3.6 Case 6 *Yang* Hénon map with $q_1 = q_2 = 0.94$

By setting $q_1 = q_2 = 0.94$ in Eq. (1), the numerical results of the fractional-degree *Yang* Hénon map are shown in Figs. 6. A phase portrait is plotted in Fig. 6(a), where $a_1 = 1.4$. Figure 6(b) and (d) are the bifurcation diagrams ofx_1. The largest Lyapunov exponent for varied $a_1 = 0$ to 1.5 is shown in Fig. 6(c). The dynamics approaches to infinity when $a_1 > 1.447$.

The first Feigenbaum's constant measures $\delta = 4.671150$, with an error percentage of 0.04 % and

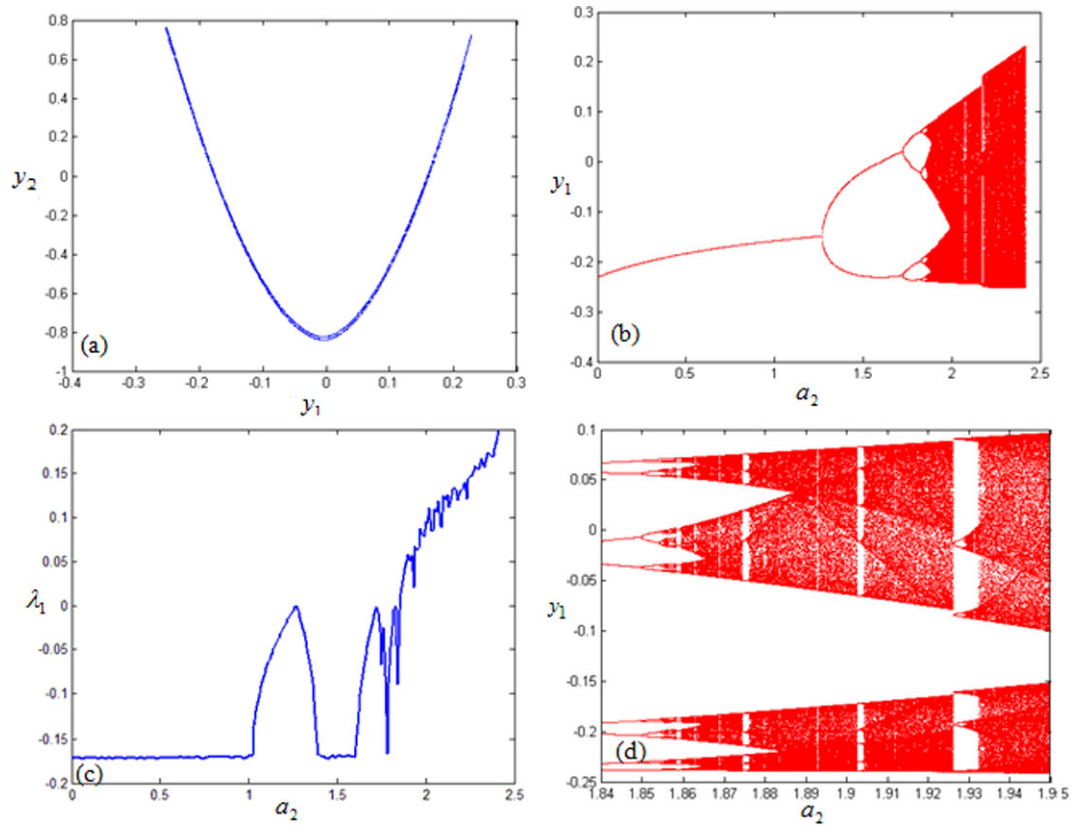

Fig. 9 The fractional-degree *Yin* Hénon map with $q_1 = 0.9$, $q_2 = 1$, $b_2 = 0.3$: (**a**) phase portrait with $a_2 = 2.4$. Bifurcation diagrams with a_2 is varied: (**b**) $0 \leq a_{2\leq} 2.5$ (**d**) $1.84 \leq a_{2\leq} 1.95$ (**c**) the largest Lyapunov exponent with $a_2 = 0 \sim 2.5$

the second Feigenbaum's constant measures $|\alpha| = 2.5036392$, with an error percentage of 0.03 % when $i = 4$.

3.7 Case 7 *Yin* Hénon map with $q_1 = q_2 = 1$

The integer degrees are $q_1 = q_2 = 1$ for the *Yin* Hénon map with decreasing n_2. The phase portrait (Fig. 7(a)), bifurcation diagrams (Figs. 7(b), (d)) and the largest Lyapunov exponent (Fig. 7(c)) show the chaotic behaviors and period-doubling bifurcations with $q_1 = q_2 = 1$. It is found that the dynamics approaches to infinity when $a_2 > 2.523$.

The first Feigenbaum's constant measures $\delta = 4.669117$, with an error percentage of 0.0017 % and the second Feigenbaum's constant measures $|\alpha| = 2.5$, with an error percentage of 0.12 % when $i = 4$.

3.8 Case 8 *Yin* Hénon map with $q_1 = 0.99$, $q_2 = 1.9$

By setting $q_1 = 0.99$, $q_2 = 1.9$ in Eq. (2), the numerical results of the fractional-degree *Yin* Hénon map are shown in Figs. 8. The largest Lyapunov exponent for varied $a_2 = 0$ to 2.2 is shown in Fig. 8(d). Figure 8(b) and (d) are the bifurcation diagrams of y_1. Various dynamic behaviors for varied a_2 can be shown by Figs. 8(b) and (d), such as the period-3 is shown when $1.869 \leq a_{1\leq} 1.884$, and the dynamics approaches to infinity when $a_2 > 2.109$.

The first Feigenbaum's constant measures $\delta = 4.677994$, with an error percentage of 0.19 % and the second Feigenbaum's constant measures $|\alpha| = 2.5053382$, with an error percentage of 0.097 % when $i = 4$.

3.9 Case 9 *Yin* Hénon map with $q_1 = 0.9$, $q_2 = 1$

By setting $q_1 = 0.9$, $q_2 = 1$ in Eq. (2), the numerical results of the fractional-degree *Yin* Hénon map

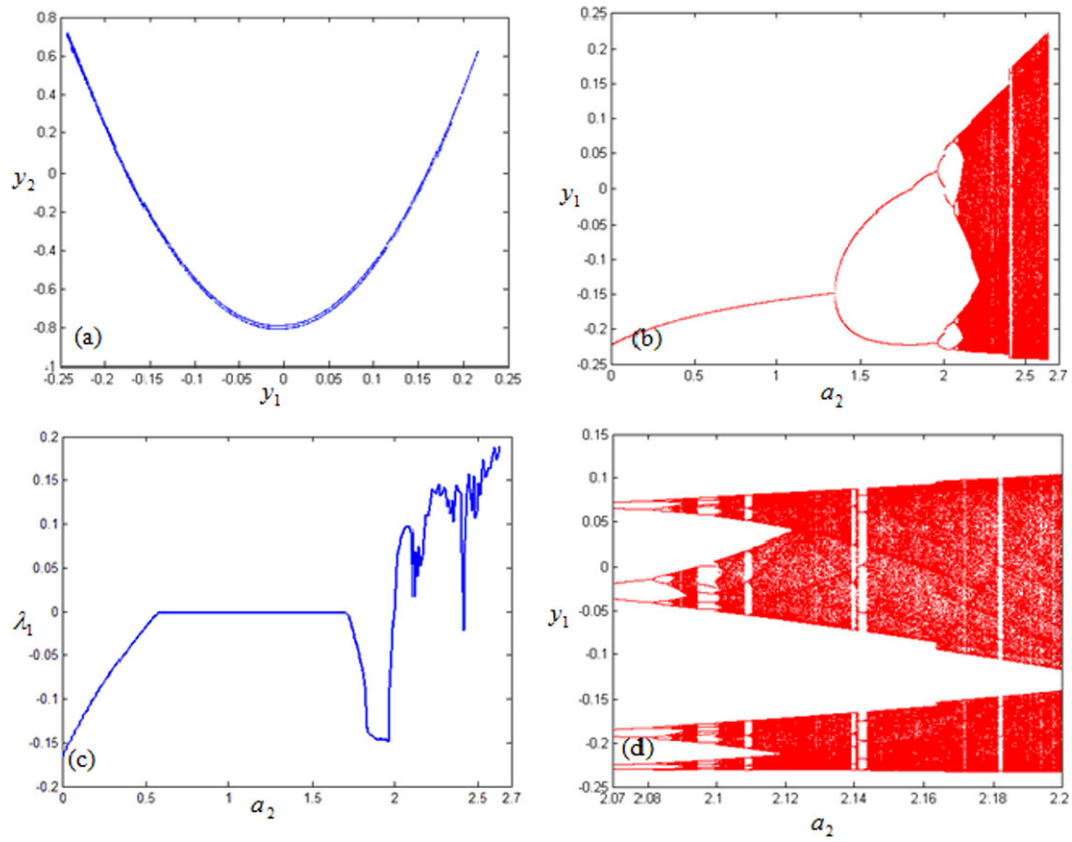

Fig. 10 The fractional-degree *Yin* Hénon map with $q_1 = 1$, $q_2 = 0.9$, $b_2 = 0.3$: (**a**) phase portrait with $a_2 = 2.6$. Bifurcation diagrams with a_2 is varied: (**b**) $0 \leq a_{2\leq} 2.7$ (**d**) $2.07 \leq a_{2\leq} 2.2$ (**c**) the largest Lyapunov exponent with $a_2 = 0 \sim 2.7$

are shown in Figs. 9. A phase portrait is plotted in Fig. 9(a), where $a_2 = 2.4$. Figure 9(b) and (d) are the bifurcation diagram of y_1, which can be shown the period-doubling bifurcations clearly. The largest Lyapunov exponent is shown in Fig. 9(c). The dynamics approaches to infinity when $a_2 > 2.413$.

The first Feigenbaum's constant measures $\delta = 4.66798$, with an error percentage of 0.026 % and the second Feigenbaum's constant measures $|\alpha| = 2.505288$, with an error percentage of 0.09 % when $i = 4$.

3.10 Case 10 *Yin* Hénon map with $q_1 = 1$, $q_2 = 0.9$

By setting $q_1 = 1$, $q_2 = 0.9$ in Eq. (2), the numerical results of the fractional-degree *Yin* Hénon map are shown in Figs. 10. A phase portrait is plotted in Fig. 10(a), where $a_2 = 2.6$. Figure 10(b) and (d) are the bifurcation diagram of y_1, which can be shown the period-doubling bifurcations clearly. The largest Lyapunov exponent is shown in Fig. 10(c). The dynamics approaches to infinity when $a_2 > 2.631$.

The first Feigenbaum's constant measures $\delta = 4.668926$, with an error percentage of 0.006 % and the second Feigenbaum's constant measures $|\alpha| = 2.504878$, with an error percentage of 0.08 % when $i = 4$.

3.11 Case 11 *Yin* Hénon map with $q_1 = q_2 = 0.98$

By setting $q_1 = q_2 = 0.98$ in Eq. (2), the numerical results of the fractional-degree *Yin* Hénon map are shown in Figs. 11. A phase portrait is plotted in Fig. 11(a), where $a_2 = 2.5$. Figure 11(b) and (d) are the bifurcation diagram of y_1, which can be shown the period-doubling bifurcations clearly. The largest Lyapunov exponent is shown in Fig. 11(c). The dynamics approaches to infinity when $a_2 > 2.519$.

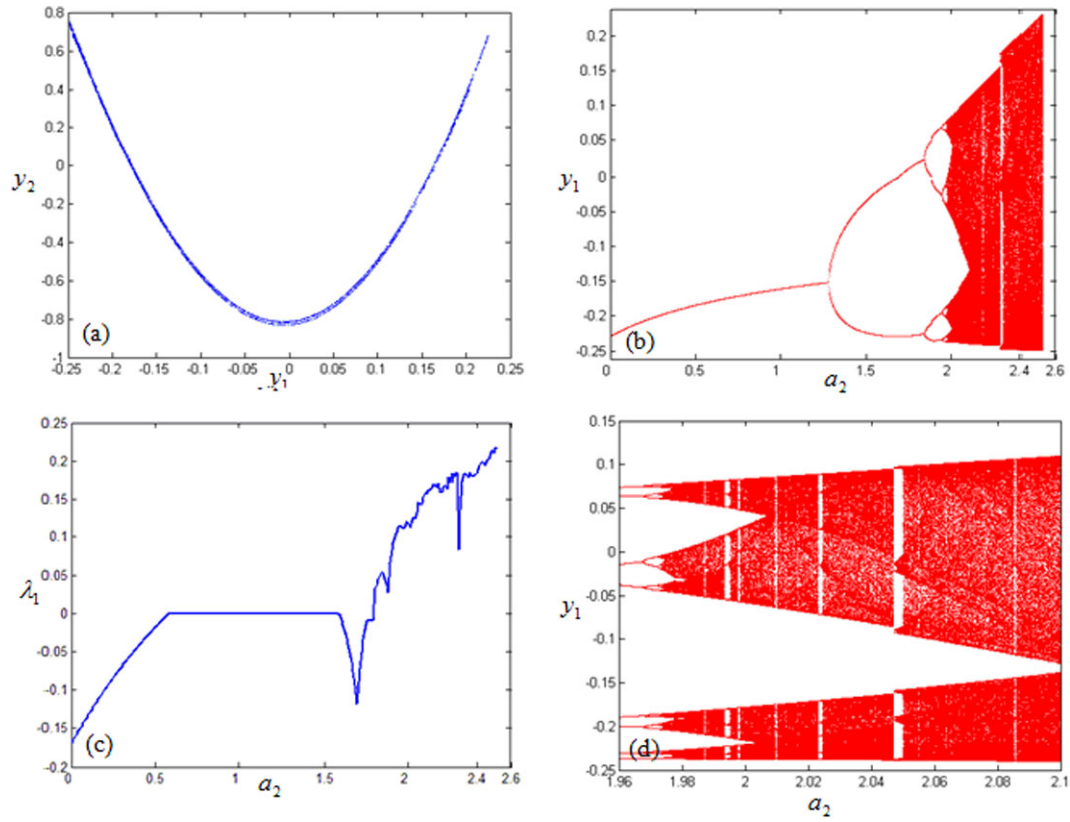

Fig. 11 The fractional-degree *Yin* Hénon map with $q_1 = q_2 = 98$, $b_2 = 0.3$: (**a**) phase portrait with $a_2 = 2.5$. Bifurcation diagrams with a_2 is varied: (**b**) $0 \leq a_2 \leq 2.6$ (**d**) $1.96 \leq a_2 \leq 2.1$ (**c**) the largest Lyapunov exponent with $a_2 = 0 \sim 2.6$

The first Feigenbaum's constant measures $\delta = 4.672820$, with an error percentage of 0.078 % and the second Feigenbaum's constant measures $|\alpha| = 2.5053072$, with an error percentage of 0.096 % when $i = 4$.

3.12 Case 12 *Yin* Hénon map with $q_1 = q_2 = 0.94$

By setting $q_1 = q_2 = 0.94$ in Eq. (2), the numerical results of the fractional-degree *Yin* Hénon map are shown in Figs. 12. A phase portrait is plotted in Fig. 12(a), where $a_2 = 2.5$. Figure 12(b) and (d) are the bifurcation diagram of y_1, which can be shown the period-doubling bifurcations clearly. The largest Lyapunov exponent for varied $a_2 = 0$ to 2.6 is shown in Fig. 12(c). The dynamics approaches to infinity when $a_2 > 2.515$.

The first Feigenbaum's constant measures $\delta = 4.690928$, with an error percentage of 0.465 % and the second Feigenbaum's constant measures $|\alpha| = 2.502722$, with an error percentage of 0.007 % when $i = 4$.

4 Conclusions

In this paper, we firstly develop the *Yin–Yang* fractional-degree Hénon maps and measure the Feigenbaum's constants to testify the existence of the chaotic behaviors on different types of q_1, q_2, which can be summarized as follows:

1. The variation of fractional degrees affects the values of bifurcation points.
2. The variation of fractional degrees affects the chaotic behaviors; Period-3 motion is found among them.
3. The measurement precision of Feigenbaum's constants is independent of q_1 and q_2, it depends on the value of i.

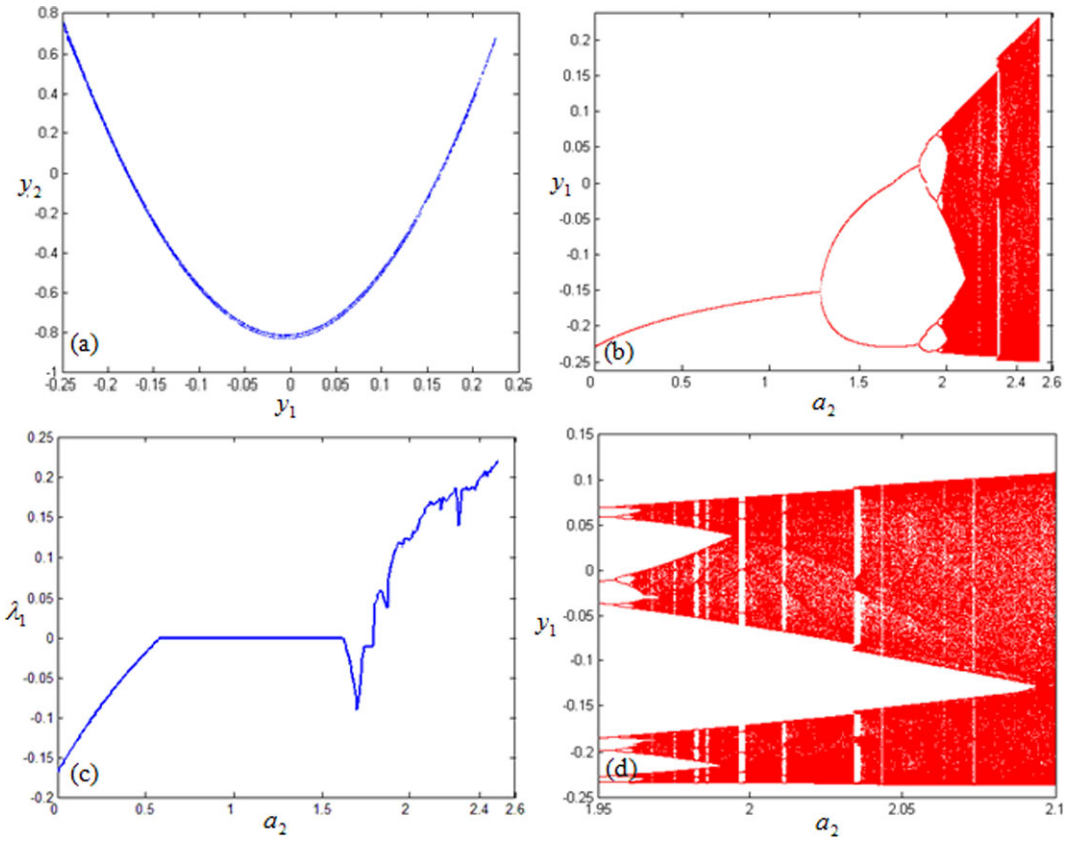

Fig. 12 The fractional-degree *Yin* Hénon map with $q_1 = q_2 = 0.94$, $b_2 = 0.3$: (**a**) phase portrait with $a_2 = 2.5$. Bifurcation diagrams with a_2 is varied: (**b**) $0 \leq a_{2\leq} 2.6$ (**d**) $1.95 \leq a_{2\leq} 2.1$ (**c**) the largest Lyapunov exponent with $a_2 = 0 \sim 2.6$

It is worthwhile to notice that further development of *Yin* and *Yang* systems for real engineering problems. The extension of the *Yin* and *Yang* concept to other kinds of nonlinear systems like fractional-order systems may produce even more interesting dynamical characteristics.

Acknowledgements The research was partially supported by a grant (NCS101-2221-E-164-008) from the National Science Council, R.O.C.

References

1. Ott, E., Grebogi, C., Yorke, J.A.: Controlling chaos. Phys. Rev. Lett. **64**, 1196–1199 (1990)
2. Pecora, L.M., Carroll, T.L.: Synchronization in chaotic systems. Phys. Rev. Lett. **64**, 821–824 (1990)
3. Arnéodo, A., Argoul, F., Elezgaray, J., Richetti, P.: Homoclinic chaos in chemical systems. Physica D **62**, 134–169 (1993)
4. Igeta, K., Ogawa, T.: Information dissipation in quantum-chaotic systems: computational view and measurement induction. Chaos Solitons Fractals **5**, 1365–1379 (1995)
5. Chen, H.K.: Global chaos synchronization of new chaotic systems via nonlinear control. Chaos Solitons Fractals **23**, 1245–1251 (2005)
6. Lu, J., Wu, X., Lü, J.: Synchronization of a unified chaotic system and the application in secure communication. Phys. Lett. A **305**, 365–370 (2002)
7. Chua, L.O., Itah, M., Kosarev, L., Eckert, K.: Chaos synchronization in Chua's circuits. J. Circuits Syst. Comput. **3**, 93–108 (1993)
8. Wiggins, S.: Introduction to Applied Nonlinear Dynamical Systems and Chaos. Springer, Berlin (2003)
9. Bao, J., Yang, Q.: Complex dynamics in the stretch-twist-fold flow. Nonlinear Dyn. **61**, 773–781 (2010)
10. Wu, W., Chen, Z.: Hopf bifurcation and intermittent transition to hyperchaos in a novel strong four-dimensional hyperchaotic system. Nonlinear Dyn. **60**, 615–630 (2010)
11. Liu, Y., Pang, W.: Dynamics of the general Lorenz family. Nonlinear Dyn. **67**, 1595–1611 (2012)
12. Śliwa, I., Grygiel, K.: Periodic orbits, basins of attraction and chaotic beats in two coupled Kerr oscillators. Nonlinear Dyn. **67**, 755–765 (2012)

13. Li, X., Ou, Q.: Dynamical properties and simulation of a new Lorenz-like chaotic system. Nonlinear Dyn. **65**, 255–270 (2011)
14. Mirzaei, O., Yaghoobi, M., Irani, H.: A new image encryption method: parallel sub-image encryption with hyper chaos. Nonlinear Dyn. **67**, 557–566 (2012)
15. Chen, C.S.: Optimal nonlinear observers for chaotic synchronization with message embedded. Nonlinear Dyn. **61**, 623–632 (2010)
16. Wang, D., Zhang, J.: Research and perspective of secure communication based on synchronization of chaos. J. Nav. Aeronaut. Eng. Inst. **21**, 257–260 (2006)
17. Wang, X.Y., Yang, L., Liu, R., Kadir, A.: A chaotic image encryption algorithm based on perceptron model. Nonlinear Dyn. **62**, 615–621 (2010)
18. Ma, J., Li, A.B., Pu, Z.S., Yang, L.J., Wang, Y.-Z.: A time-varying hyperchaotic system and its realization in circuit. Nonlinear Dyn. **62**, 535–541 (2010)
19. Chen, Z., Ip, W.H., Chan, C.Y., Yung, K.L.: Two-level chaos-based video cryptosystem on H.263 codec. Nonlinear Dyn. **62**, 647–664 (2010)
20. Chen, G., Dong, X.: From Chaos to Order: Methodologies, Perspectives and Applications. World Scientific, Singapore (1988)
21. Hénon, M.: A two-dimensional mapping with a strange attractor. Commun. Math. Phys. **50**, 69–77 (1976)
22. Lorenz, E.N.: Compound windows of the Hénon map. Physica D **237**, 1689–1704 (2008)
23. Sterling, D., Dullin, H.R., Meiss, J.D.: Homoclinic bifurcations for the Hénon map. Physica D **134**, 153–184 (1999)
24. Feigenbaum, M.J.: Quantitative universality for a class of nonlinear transformations. J. Stat. Phys. **19**, 25–52 (1978)
25. Feigenbaum, M.J.: Universal behavior in nonlinear systems. Los Alamos Sci. **1**, 4–27 (1980)
26. Goldfain, E.: Feigenbaum scaling, Cantorian space-time and the hierarchical structure of standard model parameters. Chaos Solitons Fractals **30**, 324–331 (2006)
27. San Martin, J.: Intermittency cascade. Chaos Solitons Fractals **32**, 816–831 (2007)
28. Letellier, C., Bennoud, M., Martel, G.: Intermittency and period-doubling cascade on tori in a bimode laser model. Chaos Solitons Fractals **33**, 782–794 (2007)
29. Chen, H.K., Sheu, L.J., Tam, L.M., Lao, S.K.: A new finding of the existence of Feigenbaum's constants in the fractional-order Chen–Lee system. Nonlinear Dyn. **68**, 589–599 (2012)
30. Ge, Z.M., Li, S.Y.: Yang and Yin parameters in the Lorenz system. Nonlinear Dyn. **62**, 105–117 (2010)
31. Ho, C.Y., Chen, H.K., Ge, Z.M.: Design of PDC controllers by matrix reversibility for synchronization of Yin and Yang chaotic Takagi–Sugeno fuzzy Hénon maps. Abstract and Applied Analysis 11 pages (2012)